Hierarchical cluster structures in a one-dimensional swarm oscillator model

Masatomo Iwasa,* Kazuki Iida,† and Dan Tanaka‡
Department of Complex Systems Science, Graduate School of Information Science, Nagoya University, Nagoya 464-8601, Japan

(Received 24 November 2009; revised manuscript received 12 February 2010; published 30 April 2010)

Swarm oscillator model derived by one of the authors (Tanaka), where interacting motile elements form various kinds of patterns, is investigated. We particularly focus on the cluster patterns in one-dimensional space. We mathematically derive all static and stable configurations in final states for a particular but a large set of parameters. In the derivation, we introduce renormalized expression of this model. We find that the static final states are hierarchical cluster structures in which a cluster consists of smaller clusters in a nesting manner.

DOI: 10.1103/PhysRevE.81.046220 PACS number(s): 05.45.−a, 05.65.+b, 45.50.−j, 61.46.Bc

I. INTRODUCTION

Cluster formation is one of the specific features in self-organizing systems. Various kinds of models exhibiting cluster structures have been proposed and analyzed to date: models for self-propelled particles which is known as Vicsek model [1–8], those with the active Brownian motion [9–14], those for deterministic dynamical systems [15–19], and a gaslike model with a coupled map [20,21]. In self-organizing systems, the existence of internal states of the elements often leads to diversity of collective behaviors because it brings about both attractive and repulsive interactions between elements.

In this paper, we focus on swarm oscillator model, which was derived by one of the authors (Tanaka) [22]. We simply refer to it as SO model in what follows. SO model has the following features. Elements each of which has an internal degree of freedom are spatially distributed. The governing equations for each element are

$$\dot{\psi}_i = \sum_{\{j|j\neq i\}} e^{-|\boldsymbol{R}_{ji}|} \sin(\Psi_{ji} + \alpha|\boldsymbol{R}_{ji}| - c_1), \quad (1)$$

$$\dot{\boldsymbol{r}}_i = c_3 \sum_{\{j|j\neq i\}} \hat{\boldsymbol{R}}_{ji} e^{-|\boldsymbol{R}_{ji}|} \sin(\Psi_{ji} + \alpha|\boldsymbol{R}_{ji}| - c_2). \quad (2)$$

Here, ψ_i (mod 2π) or $\boldsymbol{r}_i$ denotes the phase or the position of the ith element, respectively. The overdot represents differentiation with respect to time. $\boldsymbol{R}_{ji} := \boldsymbol{r}_j - \boldsymbol{r}_i$, $\hat{\boldsymbol{R}}_{ji} := \boldsymbol{R}_{ji}/|\boldsymbol{R}_{ji}|$, and $\Psi_{ji} := \psi_j - \psi_i$. From the physical point of view, we can regard the phase as a simple representation of an internal state of an element such as magnetic or electric polarity of an atom or a molecule, molecular geometry, or a state of bacterium or a cell. This model has four real parameters, $0 \le c_1 < 2\pi$, $0 \le c_2 < 2\pi$, $0 \le c_3$, and $0 \le \alpha$. Compared with models in previous studies, this model can be regarded as an extended nonlocally coupled motile phase-oscillator model [23–26] because of the interaction between elements with sinusoidal functions. The sinusoidal functions include phase shifts, c_1 and c_2. It has been found that nonzero phase shifts break odd symmetries of coupling functions and cause rich structures or patterns in phase-oscillator systems [27–29]. It should be noted that this model has the following physical background [22]. Here we review it briefly. It is assumed that elements are spatially distributed in a chemical field that diffuses in space. Each element in isolation has a self-sustained dynamical system. The internal dynamics is characterized by a supercritical Hopf bifurcation above which exhibits oscillatory dynamics. The motion of each element is driven by the local gradient of the chemical density, and the elements produce and consume this chemical in amounts that depend on their internal states. From this general model for chemotactic oscillators, SO model is derived by means of the center-manifold reduction and the phase reduction [23]. In short, SO model describes an asymptotic behavior of the above system for chemotactic oscillators. In spite of the simplicity of the equations, this model exhibits a rich variety of ordered structures depending on the four parameter values, the number of elements N, and the system size L. Some results of numerical simulations are shown in Fig. 1. Judging from this richness, it can be inferred that this model holds mathematical structures which underlie various collective behaviors. Therefore, analyzing this model in detail seems to be significant to understand the mechanism or essential factors of various kinds of structure formations.

Among patterns SO model exhibits, we concentrate on cluster patterns in this paper. SO model is unique in the point that elements form clustered cluster structures, that is, a large cluster consists of some smaller clusters (bottom-left figure in Fig. 1). To comprehend the behavior mathematically and analytically, considering a simpler model is one of the best strategies. In this paper, we investigate a particular type of one-dimensional SO model. As a result, we analytically derive all of the static configurations of the elements and identify all cluster structures in final states of the one-dimensional model for a particular but a large set of parameters.

II. MODEL

This paper investigates a specific type of one-dimensional swarm oscillator model, which is the following system of ordinary differential equations:

*miwasa@r.phys.nagoya-u.ac.jp
†Also at Department of Human and Artificial Intelligent Systems, Graduate School of Engineering, University of Fukui.
‡Also at Precursory Research for Embryonic Science and Technology (PRESTO), Japan Science and Technology Agency (JST).

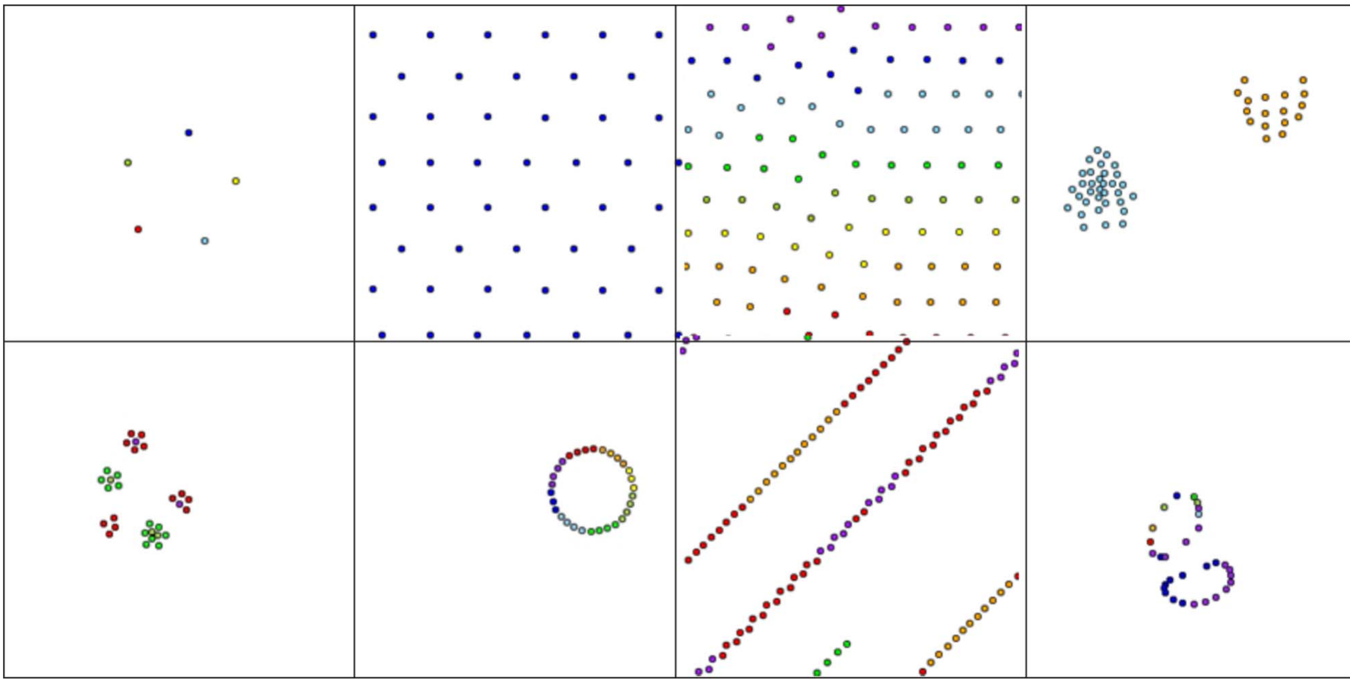

FIG. 1. (Color online) Examples of spatial patterns exhibited by swarm oscillator model in two-dimensional space. Color (grayscale) represents the phase of oscillators. Some are static states and others are steadily moving states.

$$\dot{\psi}_i = \sum_{j\neq i} e^{-|R_{ji}|} \sin(\Psi_{ji} + \alpha|R_{ji}| - c), \quad (3)$$

$$\dot{r}_i = c_3 \sum_{j\neq i} \frac{R_{ji}}{|R_{ji}|} e^{-|R_{ji}|} \sin(\Psi_{ji} + \alpha|R_{ji}| - c). \quad (4)$$

Here, $\psi_i (\mathrm{mod}\ 2\pi)$ or r_i $(i=1,2,\ldots,N)$ denotes the phase or the position of the ith element, respectively. N is the total number of elements. The overdot represents differentiation with respect to time. $R_{ji} := r_j - r_i$ and $\Psi_{ji} := \psi_j - \psi_i$. c_3 and α are positive parameters, and $0 \leq c < 2\pi$. The system size is finite but large enough. Note that Eqs. (3) and (4) are a particular type of Eqs. (1) and (2), with $c_1 = c_2 =: c$ in one-dimensional space. Next, we introduce valuables, $\theta_i := \psi_{i+1} - \psi_i$ (mod 2π) and $\rho_i := r_{i+1} - r_i$, $(i=1,2,\ldots,N-1)$. As long as we focus on the long-time behavior where elements are almost static, we can assume $\rho_i \geq 0$ without loss of generality. Then, Eqs. (3) and (4) become

$$\dot{\psi}_i = \sum_{j=1}^{i-1} e^{-\sum_{k=j}^{i-1}\rho_k} \sin\left(\alpha \sum_{k=j}^{i-1} \rho_k - \sum_{k=j}^{i-1} \theta_k - c\right) + \sum_{j=i}^{N-1} e^{-\sum_{k=i}^{j}\rho_k} \sin\left(\alpha \sum_{k=i}^{j} \rho_k + \sum_{k=i}^{j} \theta_k - c\right), \quad (5)$$

$$\dot{r}_i = -c_3 \sum_{j=1}^{i-1} e^{-\sum_{k=j}^{i-1}\rho_k} \sin\left(\alpha \sum_{k=j}^{i-1} \rho_k - \sum_{k=j}^{i-1} \theta_k - c\right) + c_3 \sum_{j=i}^{N-1} e^{-\sum_{k=i}^{j}\rho_k} \sin\left(\alpha \sum_{k=i}^{j} \rho_k + \sum_{k=i}^{j} \theta_k - c\right). \quad (6)$$

This dynamical system has the following characteristic, which is useful for analysis of this model.

Proposition. For the dynamical system [Eqs. (5) and (6)], $\dot{\psi}_1 = \cdots = \dot{\psi}_N = \dot{r}_1 = \cdots = \dot{r}_N = 0 \Leftrightarrow \dot{\theta}_1 = \cdots = \dot{\theta}_{N-1} = \dot{\rho}_1 = \cdots = \dot{\rho}_{N-1} = 0$. That is to say, all fixed points of the dynamical system constituted by $\{\rho_i\}$ and $\{\theta_i\}$ represent static states with respect to positions $\{r_i\}$ and phases $\{\psi_i\}$.

Proof. $\Rightarrow$ is trivial. We show $\Leftarrow$. Since $\dot{\theta}_i = 0$ and $\dot{\rho}_i = 0$ for all i, $\dot{\psi}_1 = \cdots = \dot{\psi}_N$ and $\dot{r}_1 = \cdots = \dot{r}_N$. According to the equations for $\dot{\psi}_1$, $\dot{\psi}_N$, $\dot{r}_1$, and $\dot{r}_N$ in Eqs. (5) and (6), we see $\dot{r}_1 = c_3 \dot{\psi}_1$ and $\dot{r}_N = -c_3 \dot{\psi}_N$. Therefore, using $c_3 \neq 0$, $\dot{\psi}_1 = \dot{\psi}_N = 0$, and $\dot{r}_1 = \dot{r}_N = 0$. Thus, $\dot{r}_1 = \cdots = \dot{r}_N = \dot{\psi}_1 = \cdots = \dot{\psi}_N = 0$. □

Some results of the numerical simulations are shown in Fig. 2. We see that hierarchical cluster structures appear, that is, several size of clusters are formed and a larger cluster consists of smaller clusters in a nesting manner.

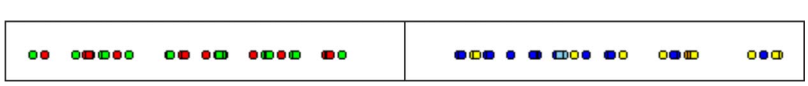

FIG. 2. (Color online) Two examples of clusters exhibited by one-dimensional SO model. The parameter values here are $c=1.0$, $c_3=1.5$, $\alpha=1.5$, $N=30$, and $L=100$. The initial conditions are such that the positions and the phases are randomly distributed. Color (grayscale) represents the phase of each element. These are final states where all positions and phases of the elements are static. Although these calculations are held with the periodic boundary condition, behavior in this system is the same as what is investigated in this paper because the system size is large enough.

III. RENORMALIZED EQUATION OF MOTION

For the sake of clear discussion in what follows, we introduce the "renormalized" expression of SO model Eqs. (3) and (4). That is,

$$\dot{\psi}_1 = A_1^+ e^{-\rho_1} \sin(\alpha\rho_1 + \theta_1 - c - \kappa_1^+), \tag{7}$$

$$\dot{r}_1 = c_3 A_1^+ e^{-\rho_1} \sin(\alpha\rho_1 + \theta_1 - c - \kappa_1^+), \tag{8}$$

$$\dot{\psi}_i = A_{i-1}^- e^{-\rho_{i-1}} \sin(\alpha\rho_{i-1} - \theta_{i-1} - c - \kappa_{i-1}^-) + A_i^+ e^{-\rho_i} \sin(\alpha\rho_i + \theta_i - c - \kappa_i^+), \tag{9}$$

$$\dot{r}_i = - c_3 A_{i-1}^- e^{-\rho_{i-1}} \sin(\alpha\rho_{i-1} - \theta_{i-1} - c - \kappa_{i-1}^-) + c_3 A_i^+ e^{-\rho_i} \sin(\alpha\rho_i + \theta_i - c - \kappa_i^+), \tag{10}$$

$$\dot{\psi}_N = A_{N-1}^- e^{-\rho_{N-1}} \sin(\alpha\rho_{N-1} - \theta_{N-1} - c - \kappa_{N-1}^-), \tag{11}$$

$$\dot{r}_N = - c_3 A_{N-1}^- e^{-\rho_{N-1}} \sin(\alpha\rho_{N-1} - \theta_{N-1} - c - \kappa_{N-1}^-), \tag{12}$$

where $i=2,\ldots,N-1$. Both A_i^- and κ_i^- $(i=1,\ldots,N-1)$ are the functions with respect to $\{\rho_1,\ldots,\rho_{i-1},\theta_1,\ldots,\theta_{i-1}\}$, and both A_i^+ and κ_i^+ $(i=1,\ldots,N-1)$ are those with respect to $\{\rho_{i+1},\ldots,\rho_{N-1},\theta_{i+1},\ldots,\theta_{N-1}\}$. Obviously, $A_1^-=A_{N-1}^+=1$ and $\kappa_1^-=\kappa_{N-1}^+=0$. The derivation of these equations is shown in the Appendix. From the physical point of view, many-body effects in this system are renormalized to $\{\kappa_i^-,\kappa_i^+,A_i^-,A_i^+\}$. That is to say, the interaction with further elements than the nearest neighbors are renormalized to $\{\kappa_i^-,\kappa_i^+,A_i^-,A_i^+\}$. Note that, if $\kappa_i^-=\kappa_i^+=0$ and $A_i^-=A_i^+=1$ for all i, these equations are the same as those constructed by taking only the interaction with the nearest-neighbor elements into consideration, what we call the nearest-neighbor approximation in what follows. With this renormalized expression of SO model, next we find fixed points, their stabilities, and, as a result, all static cluster states.

IV. FIXED POINTS

Let us find fixed points of this system. The fixed points are the solutions of the algebraic equations, $\dot{\psi}_i=\dot{r}_i=0$, which read as

$$\sin(\alpha\rho_i - \theta_i - c - \kappa_i^-) = 0, \tag{13}$$

$$\sin(\alpha\rho_i + \theta_i - c - \kappa_i^+) = 0,$$

$$\text{for} \quad i = 1,\ldots,N-1. \tag{14}$$

Then, there are two types of fixed points. One of them is formally written as

$$\rho_i = \frac{1}{2\alpha}[2c + 2n_i\pi + \kappa_i^+ + \kappa_i^-], \tag{15}$$

$$\theta_i = \frac{1}{2}(\kappa_i^+ - \kappa_i^-) \quad \text{or} \quad \theta_i = \frac{1}{2}(\kappa_i^+ - \kappa_i^-) + \pi. \tag{16}$$

The other is

$$\rho_i = \frac{1}{2\alpha}[2c + (2n_i+1)\pi + \kappa_i^+ + \kappa_i^-], \tag{17}$$

$$\theta_i = \frac{1}{2}(\kappa_i^+ - \kappa_i^-) + \frac{\pi}{2} \quad \text{or} \quad \theta_i = \frac{1}{2}(\kappa_i^+ - \kappa_i^-) + \frac{3\pi}{2}. \tag{18}$$

Here n_i is an integer which satisfies $\rho_i>0$. We refer to the former type or the latter type as type (I) or type (II), respectively. If we self-consistently solve these equations with respect to $\{\rho_i\}$ and $\{\theta_i\}$, we obtain the distances and the phase differences between elements in principle. Although construction of exact solutions is difficult by analytical calculations, we can approximately find the distances and the phase differences including many-body effects under the condition

$$\frac{2c + n_0\pi}{2\alpha} \gtrsim 1. \tag{19}$$

Here n_0 denotes the minimal integer which satisfies $2c+n_0\pi>0$. Then, both κ_i^- and κ_i^+ are small enough compared with 1, and A_i^- and A_i^+ are nearly equal to 1 for all i, in terms of the results in the Appendix. This condition holds except special case, $\alpha\gg 1$, $c\simeq\frac{\pi}{2}$, or $c\simeq\frac{3\pi}{2}$. Therefore, each distance between adjacent elements takes discrete values labeled by an integer n_i. Note that, since the nearest-neighbor analysis is the same as that for the case of $\kappa_i^+=\kappa_i^-=0$ for all i, each static configuration of elements can be corresponded to one of the static configurations for the nearest-neighbor approximation.

V. LINEAR STABILITY ANALYSIS

By means of the linear stability analysis, let us find configurations of elements which can finally emerge under the above condition. It is shown that the stability of each fixed point is the same as that with the nearest-neighbor approximation as follows. Here we particularly consider fixed points of type (I). As we remark later again, note that we can discuss for type (II) in the same manner. Let $\{\rho_0,\theta_0\}$ be a fixed point of the full dynamics of SO model, that is to say,

$$\sin(\alpha\rho_{0i} - \theta_{0i} - c - \kappa_{0i}^-) = 0, \tag{20}$$

$$\sin(\alpha\rho_{0i} + \theta_{0i} - c - \kappa_{0i}^+) = 0,$$

$$\text{for} \quad i = 1,\ldots,N-1. \tag{21}$$

Then, for $\theta_i=:\theta_{0i}+\tilde{\theta}_i$ and $\rho_i=:\rho_{0i}+\tilde{\rho}_i$, we obtain the following linearized equations:

$$\dot{\theta}_i = \dot{\psi}_{i+1} - \dot{\psi}_i = A_i^- e^{-\rho_i}\sin(\alpha\rho_i - \theta_i - c - \kappa_i^-) + A_{i+1}^+ e^{-\rho_{i+1}}\sin(\alpha\rho_{i+1} + \theta_{i+1} - c - \kappa_{i+1}^+) - A_{i-1}^- e^{-\rho_{i-1}}\sin(\alpha\rho_{i-1} - \theta_{i-1} - c - \kappa_{i-1}^-) - A_i^+ e^{-\rho_i}\sin(\alpha\rho_i + \theta_i - c - \kappa_i^+), \tag{22}$$

$$\dot{\tilde{\theta}}_i = A_{0i}^- e^{-\rho_{0i}}\sigma_i\left[\alpha\tilde{\rho}_i - \tilde{\theta}_i - \sum_k \left.\frac{\partial\kappa_i^-}{\partial\theta_k}\right|_0 \tilde{\theta}_k - \sum_k \left.\frac{\partial\kappa_i^-}{\partial\rho_k}\right|_0 \tilde{\rho}_k\right] + A_{0i+1}^+ e^{-\rho_{0i+1}}\sigma_{i+1}\left[\alpha\tilde{\rho}_{i+1} + \tilde{\theta}_{i+1} - \sum_k \left.\frac{\partial\kappa_{i+1}^+}{\partial\theta_k}\right|_0 \tilde{\theta}_k - \sum_k \left.\frac{\partial\kappa_{i+1}^+}{\partial\rho_k}\right|_0 \tilde{\rho}_k\right] - A_{0i-1}^- e^{-\rho_{0i-1}}\sigma_{i-1}\left[\alpha\tilde{\rho}_{i-1} - \tilde{\theta}_{i-1} - \sum_k \left.\frac{\partial\kappa_{i-1}^-}{\partial\theta_k}\right|_0 \tilde{\theta}_k - \sum_k \left.\frac{\partial\kappa_{i-1}^-}{\partial\rho_k}\right|_0 \tilde{\rho}_k\right] - A_{0i}^+ e^{-\rho_{0i}}\sigma_i\left[\alpha\tilde{\rho}_i + \tilde{\theta}_i - \sum_k \left.\frac{\partial\kappa_i^+}{\partial\theta_k}\right|_0 \tilde{\theta}_k - \sum_k \left.\frac{\partial\kappa_i^+}{\partial\rho_k}\right|_0 \tilde{\rho}_k\right] + \mathrm{O}(\{\tilde{\rho}_i^2\},\{\tilde{\rho}_i\tilde{\theta}_i\},\{\tilde{\theta}_i^2\}), \tag{23}$$

where $|_0$ denotes the substitution of (ρ_0,θ_0) after differentiation, and $\sigma_i := \cos(\alpha\rho_{0i} - \theta_{0i} - c - \kappa_{i0}^-) = \cos(\alpha\rho_{0i} + \theta_{0i} - c - \kappa_{i0}^+) = 1$ or -1 for fixed points of type (I). In the same way, we obtain

$$\dot{\rho}_i = \dot{r}_{i+1} - \dot{r}_i = -A_i^- e^{-\rho_i}\sin(\alpha\rho_i - \theta_i - c - \kappa_i^-) + A_{i+1}^+ e^{-\rho_{i+1}}\sin(\alpha\rho_{i+1} + \theta_{i+1} - c - \kappa_{i+1}^+) + A_{i-1}^- e^{-\rho_{i-1}}\sin(\alpha\rho_{i-1} - \theta_{i-1} - c - \kappa_{i-1}^-) - A_i^+ e^{-\rho_i}\sin(\alpha\rho_i + \theta_i - c - \kappa_i^-), \tag{24}$$

$$\dot{\tilde{\rho}}_i = -A_{0i}^- e^{-\rho_{0i}}\sigma_i\left[\alpha\tilde{\rho}_i - \tilde{\theta}_i - \sum_k \left.\frac{\partial\kappa_i^-}{\partial\theta_k}\right|_0 \tilde{\theta}_k - \sum_k \left.\frac{\partial\kappa_i^-}{\partial\rho_k}\right|_0 \tilde{\rho}_k\right] + A_{0i+1}^+ e^{-\rho_{0i+1}}\sigma_{i+1}\left[\alpha\tilde{\rho}_{i+1} + \tilde{\theta}_{i+1} - \sum_k \left.\frac{\partial\kappa_{i+1}^+}{\partial\theta_k}\right|_0 \tilde{\theta}_k - \sum_k \left.\frac{\partial\kappa_{i+1}^+}{\partial\rho_k}\right|_0 \tilde{\rho}_k\right] + A_{0i-1}^- e^{-\rho_{0i-1}}\sigma_{i-1}\left[\alpha\tilde{\rho}_{i-1} - \tilde{\theta}_{i-1} - \sum_k \left.\frac{\partial\kappa_{i-1}^-}{\partial\theta_k}\right|_0 \tilde{\theta}_k - \sum_k \left.\frac{\partial\kappa_{i-1}^-}{\partial\rho_k}\right|_0 \tilde{\rho}_k\right] - A_{0i}^+ e^{-\rho_{0i}}\sigma_i\left[\alpha\tilde{\rho}_i + \tilde{\theta}_i - \sum_k \left.\frac{\partial\kappa_i^+}{\partial\theta_k}\right|_0 \tilde{\theta}_k - \sum_k \left.\frac{\partial\kappa_i^+}{\partial\rho_k}\right|_0 \tilde{\rho}_k\right] + \mathrm{O}(\{\tilde{\rho}_i^2\},\{\tilde{\rho}_i\tilde{\theta}_i\},\{\tilde{\theta}_i^2\}). \tag{25}$$

Thus, it has been shown that, since $\partial_\theta\kappa|_0$, $\partial_\rho\kappa|_0$, and $A_0 - 1$ are small as mentioned before, the stability of a fixed point $\{\theta_0,\rho_0\}$ is the same as the corresponding one in the nearest-neighbor analysis for the same $\{n_i\}$ introduced in Eq. (15).

Then, we have only to investigate the linear stability for the nearest-neighbor model to obtain the stability of fixed points of the exact SO model. The linearized differential equations of the nearest-neighbor model become

$$\dot{\tilde{\theta}}_i = -e^{-\rho_{0i-1}}\sigma_{i-1}(\alpha\tilde{\rho}_{i-1} - \tilde{\theta}_{i-1}) - 2e^{-\rho_{0i}}\sigma_i\tilde{\theta}_i + e^{-\rho_{0i+1}}\sigma_{i+1}(\alpha\tilde{\rho}_{i+1} + \tilde{\theta}_{i+1}), \tag{26}$$

$$\dot{\tilde{\rho}}_i = c_3 e^{-\rho_{0i-1}}\sigma_{i-1}(\alpha\tilde{\rho}_{i-1} - \tilde{\theta}_{i-1}) - 2\alpha c_3 e^{-\rho_{0i}}\sigma_i\tilde{\rho}_i + c_3 e^{-\rho_{0i+1}}\sigma_{i+1}(\alpha\tilde{\rho}_{i+1} + \tilde{\theta}_{i+1}). \tag{27}$$

By means of ordinary eigenvalue analysis, we find that fixed points are stable if and only if they satisfy $\sigma_i = 1$ for all i.

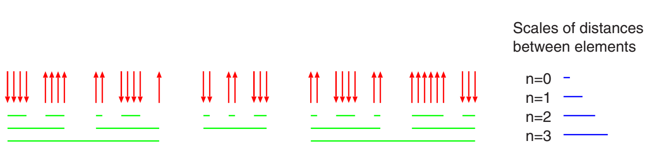

FIG. 3. (Color online) The schematic illustration of an example of hierarchical cluster structures arising in final states of SO model. Directions of arrows represent the phases of oscillators. Lines under the arrows indicate the units of components of clusters. We can find that small clusters make up larger clusters and those make up further larger clusters.

This means that, when the distance between any pair of adjacent particles takes the value labeled by even n_i or odd n_i, the phase difference takes nearly 0 or π, respectively. Note that this stability condition corresponds with that for the two-body system [30].

In contrast, we can show that all fixed points of type (II) are not stable in the same manner, noting that $\cos(\alpha\rho_{0i} - \theta_{0i} - c - \kappa_{0i}^-) = -\cos(\alpha\rho_{0i} + \theta_{0i} - c - \kappa_{0i}^+)$ holds for type (II) fixed points while $\cos(\alpha\rho_{0i} - \theta_{0i} - c - \kappa_{0i}^-) = \cos(\alpha\rho_{0i} + \theta_{0i} - c - \kappa_{0i}^+)$ for type (I).

As a consequence, we have derived all static stable configurations of elements under the condition Eq. (19). For example, if $0 < c < \frac{\pi}{2}$, the minimum clusters consist of elements between which the distances are labeled by $n=0$ where the phases of those elements are almost the same. The second smallest clusters consist of those minimum clusters all of which are placed apart from another in the distance labeled by $n=1$. Then the phase differences between them are almost π. In a nesting manner, we find that hierarchical cluster structures emerge (see Fig. 3).

VI. EXAMPLE: THREE ELEMENTS

Let us consider SO model for three elements. The equations of motion become

$$\dot{\psi}_1 = e^{-\rho_1}\sin(\alpha\rho_1 + \theta_1 - c) + e^{-\rho_1-\rho_2}\sin[\alpha(\rho_1+\rho_2) + (\theta_1+\theta_2) - c], \tag{28}$$

$$=: A_1^+ e^{-\rho_1}\sin(\alpha\rho_1 + \theta_1 - c - \kappa_1^+), \tag{29}$$

$$\dot{\psi}_2 = e^{-\rho_1}\sin(\alpha\rho_1 - \theta_1 - c) + e^{-\rho_2}\sin(\alpha\rho_2 + \theta_2 - c), \tag{30}$$

$$\dot{\psi}_3 = e^{-\rho_1-\rho_2}\sin[\alpha(\rho_1+\rho_2) - (\theta_1+\theta_2) - c] + e^{-\rho_2}\sin(\alpha\rho_2 - \theta_2 - c), \tag{31}$$

$$=: A_2^- e^{-\rho_2}\sin(\alpha\rho_2 - \theta_2 - c - \kappa_2^-), \tag{32}$$

$$\dot{r}_1 = A_1^+ e^{-\rho_1}\sin(\alpha\rho_1 + \theta_1 - c - \kappa_1^+), \tag{33}$$

$$\dot{r}_2 = -e^{-\rho_1}\sin(\alpha\rho_1 - \theta_1 - c) + e^{-\rho_2}\sin(\alpha\rho_2 + \theta_2 - c), \tag{34}$$

$$\dot{r}_3 = -A_2^- e^{-\rho_2}\sin(\alpha\rho_2 - \theta_2 - c - \kappa_2^-), \tag{35}$$

where

$$\sin\kappa_i^{\pm} := \frac{-\sigma_{i\pm1}^{\pm} e^{-\rho_{i\pm1}}\sin c}{A_i^{\pm}}, \tag{36}$$

$$\cos\kappa_i^{\pm} := \frac{1 + \sigma_{i\pm1}^{\pm} e^{-\rho_{i\pm1}}\cos c}{A_i^{\pm}}, \tag{37}$$

$$A_i^{\pm} := [1 + \sigma_{i\pm1}^{\pm} 2 e^{-\rho_{i\pm1}}\cos c + e^{-2\rho_{i\pm1}}]^{1/2}, \tag{38}$$

$$\sigma_i^{\pm} := \cos(\alpha\rho_i \pm \theta_i - c). \tag{39}$$

Firstly, we find fixed points of this system. Fixed points satisfy the following equations:

$$\sin(\alpha\rho_1 - \theta_1 - c) = 0, \tag{40}$$

$$\sin(\alpha\rho_2 - \theta_2 - c - \kappa_2^-) = 0, \tag{41}$$

$$\sin(\alpha\rho_1 + \theta_1 - c - \kappa_1^+) = 0, \tag{42}$$

$$\sin(\alpha\rho_2 + \theta_2 - c) = 0. \tag{43}$$

Then, $\sigma_i^+ = \sigma_i^- =: \sigma_i = 1$ or -1. With the result of the linear stability analysis in the previous section, stable fixed points are formally written as follows for a set of integers (n_1, n_2):

$$(\rho_1, \theta_1) = \left[\frac{1}{\alpha}\left(c + 2n_1\pi + \frac{1}{2}\kappa_1^+\right), \frac{1}{2}\kappa_1^+\right] \tag{44}$$

$$\text{or} \quad \left\{\frac{1}{\alpha}\left[c + (2n_1+1)\pi + \frac{1}{2}\kappa_1^+\right], \pi + \frac{1}{2}\kappa_1^+\right\}, \tag{45}$$

$$(\rho_2, \theta_2) = \left[\frac{1}{\alpha}\left(c + 2n_1\pi + \frac{1}{2}\kappa_2^-\right), -\frac{1}{2}\kappa_2^-\right] \tag{46}$$

$$\text{or} \quad \left\{\frac{1}{\alpha}\left[c + (2n_2+1)\pi + \frac{1}{2}\kappa_2^-\right], \pi - \frac{1}{2}\kappa_2^-\right\}. \tag{47}$$

Next, let us estimate the distances and the phase differences between elements. Considering Eqs. (36) and (37) and noting that $\sigma_i = 1$ is the stability condition, we approximately obtain

$$\kappa_1^+ = -e^{-1/\alpha[c+2n_2\pi]}\sin c, \quad \text{or} \quad -e^{-1/\alpha[c+(2n_2+1)\pi]}\sin c, \tag{48}$$

$$\kappa_2^- = -e^{-1/\alpha[c+2n_1\pi]}\sin c, \quad \text{or} \quad -e^{-1/\alpha[c+(2n_1+1)\pi]}\sin c. \tag{49}$$

By direct substitution to Eqs. (44)–(47), we obtain the distances and the phase differences between elements approximately.

VII. CONCLUDING REMARKS

A particular type of one-dimensional swarm oscillator model has been studied in this paper. As a result, all static cluster structures emerging in final states have been identified. It has been found that this model exhibits hierarchical cluster structures. In the derivation, renormalization procedure effectively works to topologically obtain the configurations of elements. It has been shown with the three-body system that, because of many-body effects, the distances between elements are slightly changed compared with the two-body SO model (the detailed discussion for the two-body system is presented in [30]). For many models presented to date, collective behaviors of finite number of dynamical elements have been studied mainly with numerical simulations. In contrast, it is shown that SO model is one of the valuable models where we can analytically understand the behavior of elements. Although no natural phenomenon which can be directly described by this model have been discovered yet, through the mathematical investigation of this model, we obtain a physically meaningful fact that the hierarchical cluster structure may appear in other systems. From the derivation, we can conclude that it may emerge in a system which has the following two factors: (i) the two-element system has a large number of stable distances (this means that, in other words in this paper, there are many stable distances which can be labeled by index $\{n_i\}$). (ii) There exist short-range interaction between elements in the system. Technologies with which we can design tiny devices or robots with making use of self-organizations, self-assemblies, or swarm intelligence are rapidly developing today [31–34]. Results of analysis here may be applicable in designing them.

Dynamical properties such as autocorrelation functions or characteristic cluster sizes seem to be interesting matter. They cannot be clarified with analytical calculation here. They will be studied with numerical calculations in the next step more generally without the constraint $c_1 = c_2$. SO model in higher-dimensional space should be studied because more kinds of patterns appear there. With numerical simulations, we have found that the hierarchical cluster structures presented in this paper also appears in two-dimensional SO model as stated in introduction. The renormalization strategy taken in this paper may be applicable in revealing ordered states in higher-dimensional space or to other models in which there is short-range interaction between elements such as Morse potential [10].

ACKNOWLEDGMENTS

D.T, acknowledges a Grant-in-Aid for Young Scientists (B), Grants No. 20740221, 2008, from the Japan Society for the Promotion of Science.

APPENDIX: THE DERIVATION OF RENORMALIZED SO MODEL

In equations of motion (5) and (6), the term proportional to $e^{-\rho_i-\cdots-\rho_{i+k}-\rho_{i+k+1}}$, is renormalized to that proportional to $e^{-\rho_i-\cdots-\rho_{i+k}}$, both of which denote the interaction between the ith element and the element on the "right" of it, as follows:

$$\begin{aligned} & e^{-\rho_i-\cdots-\rho_{i+k}} \sin[\alpha(\rho_i+\cdots+\rho_{i+k})+\theta_i+\cdots+\theta_{i+k}-c] \\ & \quad + Ae^{-\rho_i-\cdots-\rho_{i+k}-\rho_{i+k+1}} \sin[\alpha(\rho_i+\cdots+\rho_{i+k}+\rho_{i+k+1}) \\ & \quad + \theta_i+\cdots+\theta_{i+k}+\theta_{i+k+1}-c-\kappa] \\ & =: A' e^{-\rho_i-\cdots-\rho_{i+k}} \sin[\alpha(\rho_i+\cdots+\rho_{i+k}) \\ & \quad + \theta_i+\cdots+\theta_{i+k}-c-\kappa'], \end{aligned} \tag{A1}$$

where

$$\begin{aligned} A' &:= [1+2Ae^{-\rho_{i+k+1}}\cos(\alpha\rho_{i+k+1}+\theta_{i+k+1}-\kappa) \\ & \quad + A^2 e^{-2\rho_{i+k+1}}]^{1/2}, \end{aligned} \tag{A2}$$

$$\cos\kappa' := [1+Ae^{-\rho_{i+k+1}}\cos(\alpha\rho_{i+k+1}+\theta_{i+k+1}-\kappa)]/A', \tag{A3}$$

$$\sin\kappa' := -Ae^{-\rho_{i+k+1}}\sin(\alpha\rho_{i+k+1}+\theta_{i+k+1}-\kappa)/A'. \tag{A4}$$

In the same manner, interactions between the ith element and elements on the "left" of it are renormalized as follows:

$$\begin{aligned} & Ae^{-\rho_{i-k-1}-\rho_{i-k}-\cdots-\rho_{i-1}} \sin[\alpha(\rho_{i-k-1}+\rho_{i-k}+\cdots+\rho_{i-1}) \\ & \quad -(\theta_{i-k-1}+\theta_{i-k}+\cdots+\theta_{i-1})-c-\kappa] \\ & \quad + e^{-\rho_{i-k}-\cdots-\rho_{i-1}} \sin[\alpha(\rho_{i-k}+\cdots+\rho_{i-1}) \\ & \quad -(\theta_{i-k}+\cdots+\theta_{i-1})-c] \\ & =: A' e^{-\rho_{i-k}-\cdots-\rho_{i-1}} \sin[\alpha(\rho_{i-k}+\cdots+\rho_{i-1}) \\ & \quad -(\theta_{i-k}+\cdots+\theta_{i-1})-c-\kappa'], \end{aligned} \tag{A5}$$

where

$$\begin{aligned} A' &:= [1+2Ae^{-\rho_{i-k-1}}\cos(\alpha\rho_{i-k-1}+\theta_{i-k-1}-\kappa) \\ & \quad + A^2 e^{-2\rho_{i-k-1}}]^{1/2}, \end{aligned} \tag{A6}$$

$$\cos\kappa' := [1+Ae^{-\rho_{i-k-1}}\cos(\alpha\rho_{i-k-1}+\theta_{i-k-1}-\kappa)]/A', \tag{A7}$$

$$\sin\kappa' := -Ae^{-\rho_{i-k-1}}\sin(\alpha\rho_{i-k-1}+\theta_{i-k-1}-\kappa)/A'. \tag{A8}$$

Repeating this procedure, we obtain the renormalized form of equations of motion Eqs. (5) and (6).

[1] T. Vicsek, A. Czirok, E. Ben-Jacob, I. Cohen, and O. Shochet, Phys. Rev. Lett. **75**, 1226 (1995).
[2] A. Czirok, M. Vicsek, and S. Vicsek, Physica A **264**, 299 (1999).
[3] A. S. Mikhailov and D. H. Zanette, Phys. Rev. E **60**, 4571 (1999).
[4] A. Czirok and T. Vicsek, Physica A **281**, 17 (2000).
[5] C. Huepe and M. Aldana, Phys. Rev. Lett. **92**, 168701 (2004).
[6] G. Gregoire and H. Chate, Phys. Rev. Lett. **92**, 025702 (2004).
[7] G. Baglietto and E. V. Albano, Phys. Rev. E **78**, 021125 (2008).
[8] C. Huepe and M. Aldana, Physica A **387**, 2809 (2008).
[9] U. Erdmann, W. Ebeling, and V. S. Anishchenko, Phys. Rev. E **65**, 061106 (2002).
[10] A. Chetverikov and J. Dunkel, Eur. Phys. J. B **35**, 239 (2003).
[11] U. Erdmann, W. Ebeling, and A. S. Mikhailov, Phys. Rev. E **71**, 051904 (2005).
[12] Y. Chuang, M. R. D'Orsogna, D. Marthaler, A. L. Bertozzi, and L. S. Chayes, Physica D **232**, 33 (2007).
[13] J. Strefler, U. Erdmann, and L. Schimansky-Geier, Phys. Rev. E **78**, 031927 (2008).
[14] Y. X. Li, R. Lukeman, and L. Edelstein-Keshet, Physica D **237**, 699 (2008).
[15] N. Shimoyama, K. Sugawara, T. Mizuguchi, Y. Hayakawa, and M. Sano, Phys. Rev. Lett. **76**, 3870 (1996).
[16] H. Levine, W. J. Rappel, and I. Cohen, Phys. Rev. E **63**, 017101 (2000).
[17] V. Gazi and K. M. Passino, IEEE Trans. Autom. Control **48**, 692 (2003).
[18] D. H. Zanette and A. S. Mikhailov, Physica D **194**, 203 (2004).
[19] M. R. D'Orsogna, Y. L. Chuang, A. L. Bertozzi, and L. S. Chayes, Phys. Rev. Lett. **96**, 104302 (2006).
[20] T. Shibata and K. Kaneko, Physica D **181**, 197 (2003).
[21] A. Parravano and L. M. Reyes, Phys. Rev. E **78**, 026120 (2008).
[22] D. Tanaka, Phys. Rev. Lett. **99**, 134103 (2007).
[23] Y. Kuramoto, *Chemical Oscillations, Waves and Turbulence* (Springer, Berlin, 1984).
[24] Y. Kuramoto, Prog. Theor. Phys. **94**, 321 (1995).
[25] S. H. Strogatz, Physica D **143**, 1 (2000).
[26] J. A. Acebrón, L. L. Bonilla, C. J. Pérez Vicente, F. Ritort, and R. Spigler, Rev. Mod. Phys. **77**, 137 (2005).
[27] H. Sakaguchi, S. Shinomoto, and Y. Kuramoto, Prog. Theor. Phys. **79**, 1069 (1988).
[28] P. J. Kim, T. W. Ko, H. Jeong, and H. T. Moon, Phys. Rev. E **70**, 065201(R) (2004).
[29] T. Aoki and T. Aoyagi, Phys. Rev. Lett. **102**, 034101 (2009).
[30] M. Iwasa and D. Tanaka (unpublished).
[31] J. Lehn, Science **295**, 2400 (2002).
[32] G. Bein, Lect. Notes Comput. Sci. **3342**, 1 (2005).
[33] A. Ishiguro and M. Shimizu, Lect. Notes Comput. Sci. **4850**, 144 (2007).
[34] M. Grunze, Nature (London) **454**, 585 (2008).